



Chemical thermodynamics of silica: a critique on its geothermometer

Mahendra P. Verma

Geotermia, Instituto de Investigaciones Electricas, Apdo. 1-475, Cuernavaca 62001, Mexico

Received 12 October 1998; accepted 14 September 1999

Abstract

The chemical thermodynamic concepts used in the calculation of solubility data of silica (quartz) are presented taking into account the PVT characteristics of water. The temperature-dependence trends between the thermodynamically calculated and the experimental quartz solubility data are very similar, but the values are widely different at high temperatures. The experimental solubility, especially along the saturation curve at high temperature and thermodynamic data for silica need to be reevaluated in order to use silica chemistry to understand geological processes. There could exist a wide range of values for silica solubility at a specified temperature, depending upon the amount of water in the reaction vessel. Thus the silica contents in geothermal fluid, in general, cannot be used as a geothermometer to estimate the reservoir temperature. The derivation of a silica geothermometer needs an extra assumption about the total amount of water in the system. The solubility data for the two extreme cases, i.e. when the vessel (bomb) is completely filled with water and when there is just enough water to make the total specific volume equal to the critical volume of water at room temperature (25°C), are considered here. These lie on the two respective straight lines of $\log(\text{SiO}_2(\text{ppm}))$ against temperature (K). The equations for the two straight lines are $\log(\text{SiO}_2(\text{ppm})) = 0.0179 T(\text{K}) - 4.3214$ and $\log \text{SiO}_2(\text{ppm}) = 0.0088 T(\text{K}) - 1.6513$, respectively. In the case of the well M-19A at Cerro Prieto, the silica concentration in the reservoir liquid is higher than the experimental solubility, but is lower than the calculated solubility value. © 2000 CNR. Published by Elsevier Science Ltd. All rights reserved.

Keywords: Chemical thermodynamics; Quartz solubility; PVT characteristics of water; Quartz geothermometer; Cerro Prieto; Mexico

E-mail address: mahendra@iie.org.mx (M.P. Verma).

1. Introduction

The solubility of a substance in an aqueous solution depends, in general, on both temperature and pressure. In some ranges of temperature or pressure the solubility gradient could be high enough to use as a geothermometer or a geobarometer, respectively. In the case of geothermal fluids, White et al. (1956) proposed for the first time that the silica content could be used as a geochemical indicator of geothermal reservoir temperature, as the silica concentration in hot springs at Steamboat, Nevada was very close to the experimental solubility of amorphous silica reported by Alexander et al. (1954) and Krauskopf (1956). Since then enormous contributions have been made to gather more evidence and to create a systematic approach for the identification of geothermal reservoir characteristics from the fluid geochemistry of silica.

Böðvarsson (1960) and Böðvarsson and Pálmason (1961) concluded that the concentration of silica in warm springs in Iceland geothermal water indicated the temperature of the underlying geothermal system. Sigvaldason (1966) concluded that the concentration of silica in deep thermal waters is controlled by quartz solubility. Mahon (1966) showed that the concentration of silica in hot water discharged from drillholes at Wairakei in New Zealand is in agreement with solubility of quartz after corrections for adiabatic steam loss. Fournier and Rowe (1966) and Fournier and Truesdell (1970) demonstrated that the solubility of quartz, rather than that of the amorphous silica, controls the silica content of hot springs at Yellowstone. Arnórsson (1970, 1975) reported that the amount of dissolved silica in thermal springs in Iceland was governed by the solubility of chalcedony below 110°C, and by quartz solubility above 180°C. Levitte and Eckstein (1979) found a good correlation between the silica concentration and the orifice temperature in the warm springs along the Jordan-Dead Sea Rift Valley in Israel. Arnórsson (1985) proposed a carbonate-silica mixing model to distinguish the boiled and non-boiled geothermal waters.

In parallel, considerable efforts have been undertaken to measure the solubility of different phases of silica and to establish theoretical ground to interpret the silica contents in natural manifestations and geothermal wells. Morey et al. (1962) plotted the quartz solubility on a plot of log dissolved silica versus the reciprocal of absolute temperature. They found that the data fell along a straight line over the temperature range 20–250°C. Fournier and coworkers have developed similar working curves for other silica phases including amorphous silica (Fournier and Rowe, 1966; Morey et al., 1964), cristobalite (Fournier and Rowe, 1962), and chalcedony (Fournier and Rowe, 1966). The effect of salts on the solubility of silica phases has been studied by many workers (Fournier and Marshall, 1983; von Damm et al., 1991; Xie and Walther, 1993, 1997). Bennett (1991) studied the quartz dissolution in organic-rich aqueous systems. Gíslason et al. (1993, 1997) found that the crystalline silica at the Earth's surface was a finely intergrown mixture of quartz and moganite.

Reed and Spycher (1984) proposed an approach to estimate the reservoir temperature by considering simultaneous temperature-dependent equilibria

between many mineral phases including quartz and the solution. This approach is further developed and applied in many geothermal systems by D'Amore et al. (1987), Tole et al. (1993) and Pang and Reed (1998).

From the experimental quartz solubility data, Fournier (1977) presented the first geothermometer in equation form. Henley et al. (1984) compiled all the existing silica geothermometers for many silica phases, including the effects of adiabatic and conductive cooling processes. Fournier and Potter (1982a) derived a polynomial equation for the quartz geothermometer using the revised quartz solubility data, that is applicable up to 330°C. Ragnarsdóttir and Walther (1983) determined the pressure dependence of quartz solubility at 250°C and concluded that pressure had significant effect on calculated quartz equilibrium temperatures from silica contents in waters from deep geothermal reservoirs. Recently, Verma and Santoyo (1997) applied a statistical data treatment method and theory of error propagation to improve the silica geothermometer equation presented initially by Fournier and Potter (1982a). They also pointed out reasons for the spread in geothermometer temperatures, including errors in the regression coefficients of the geothermometric equations, accuracy and precision of the analytical determinations of chemical species in a given sample, sampling errors, calibration errors of the geothermometers for high-temperature hydrothermal systems, and errors related to the geologic and thermodynamic processes of the chemical equilibria involved in the reactions. However, the chemical thermodynamics of silica solutions is of prime importance in assessing the feasibility and applicability of silica geothermometry in geological hydrothermal systems.

The use of silica geothermometers is at present an integral part of almost all the geochemical investigations of geothermal systems around the world. Being such an important facet of geothermal energy resource development, it justifies highlighting the fundamental aspects of silica solubility and discussing the merits of its use in geothermometry. It has been well established by now that the fluids in most of the high-temperature geothermal reservoirs have sufficient residence time to attain equilibrium with quartz. The present work therefore, is focused on a chemical thermodynamic theoretical approach for calculating the solubility of quartz and comparing the calculated values with the experimental solubility data available in the literature. The derivation of the quartz geothermometer equation and the limitations of its use in geothermal systems will also be discussed. The application of this approach is elucidated in the case of the Cerro Prieto geothermal system.

2. PVT characteristics of water during solubility determination experiments

In the solubility experiment a certain amount of water and silica is closed in a reaction vessel (or bomb) and the system is heated to a certain temperature. To understand the effects of heating on the thermodynamic state of such systems, an acquaintance with the PVT characteristics of water is helpful. For the purpose of

discussing PVT characteristics of water during such experiments, let us assume that there is only water in the vessel. The amount of water determines whether there will be only liquid and/or vapor in the vessel on heating to high temperature (Smith and van Ness, 1975; Verma, 1997). For example, assume that the amount of water is such that it makes a total specific volume of $10.0 \text{ cm}^3/\text{g}$ (i.e. the total volume of container divided by the total weight (mass) of water and vapor). As we start the experiment at the environmental conditions, the initial pressure and temperature could be considered as 0.1 MPa and 25°C , respectively. So there will be compressed liquid from 25 to 100°C . As we pass the temperature 100°C , there will be vapor and liquid along the water–vapor saturation curve. On continued heating there will be more and more vapor. When the temperature reaches approximately 344°C (see steam tables by Haar et al., 1984), all the water will convert into vapor and there will be vapor only beyond this temperature. Thus there will not be any solution of silica in this case above 344°C . On the other hand, if the amount of water is such that it makes a total specific volume of $2.5 \text{ cm}^3/\text{g}$, there will be a two-phase region between 100 and 370°C and only liquid after 370°C .

Fig. 1 shows the P – T relations for water along different isochores. These curves

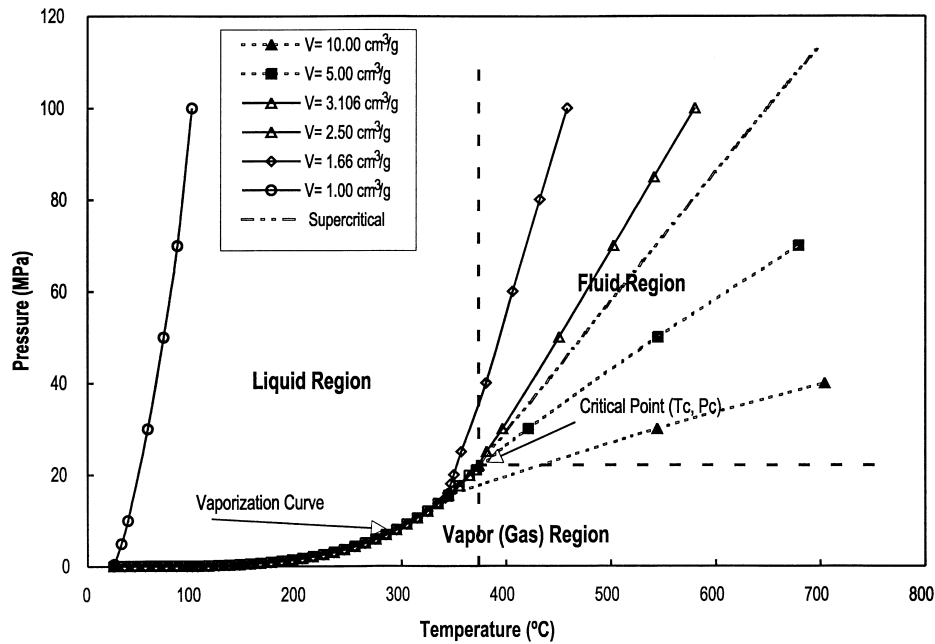


Fig. 1. The P – T characteristics of water for different total specific volumes in a closed vessel. The region above the critical point pressure (P_c) and temperature (T_c) is known as the fluid (supercritical) region. The line corresponding to the “supercritical” represents the extension of the P – T curve for the case when the specific volume is equal to the critical volume (i.e. $V = 3.106 \text{ cm}^3/\text{g}$) in the supercritical region.

have been constructed using the steam tables of Haar et al. (1984). The values for pressure and temperature are chosen so that the total specific volume on each curve is fixed to the noted value. The curve for which the total specific volume is greater than the critical specific volume of water ($3.106 \text{ cm}^3/\text{g}$) follows the water–vapor saturation curve above 100°C and at a certain temperature a path in the superheated vapor region. When the total specific volume is lower than the critical specific volume, the curves end in a compressed liquid region at higher temperatures. On continued heating, the pressure and temperature will increase and the system may reach the supercritical region (for example, see the curves corresponding to $V = 1.66$ and $2.50 \text{ cm}^3/\text{g}$ in Fig. 1). But there will definitely be compressed liquid in the reaction vessel even in the supercritical region. If the vessel is completely filled initially, the system will always be in the compressed-liquid region during such experiments.

On the other hand, if the total specific volume of water in the vessel is just equal to the critical volume of water there will be water and vapor along the water–vapor saturation curve up to the critical point. After the critical point there will not be any distinction between water and vapor along the $V = 3.106 \text{ cm}^3/\text{g}$ path, but there will be compressed liquid at any point above this line and superheated vapor below it.

Above the critical pressure and temperature the region is known as the fluid (supercritical) region, which is marked off by the thick solid dashed lines in Fig. 1. The fluid region does not represent any phase change from liquid or from vapor (Smith and van Ness, 1975). A supercritical fluid is not a single phase. There will be no phase change if a system moves from the liquid region to the fluid region unless it crosses the vaporization curve or the extended dashed and dotted line in the fluid region. It is interesting to note that if a system passes from the liquid region to the gas region across the extended dashed and dotted line, the phase change will be gradual while an abrupt phase change takes place across the vaporization curve.

In summary, there will be only vapor at high temperature if the total specific volume is greater than the critical specific volume of water, and vice versa. In the middle temperature region, however, there could be both liquid and vapor phases along the water–vapor saturation curve. At high temperature along the saturation curve, the specific volumes of vapor and water are of the same order of magnitude; the proportion of liquid (water) and vapor in the reaction vessel at each condition of temperature and pressure even above the critical condition, is therefore fundamental for accurate measurement of silica solubility.

3. Thermodynamic calculation of silica solubility

Silica is found naturally in many stable phases including quartz, chalcedony, tridymite, cristobalite, coesite, stishovite and amorphous silica. The dissolution–precipitation equilibration of such multi-phase minerals depends upon the solution–mineral contact time, and its definition requires an understanding of

mineral solubility kinetics (Stumm and Morgan, 1981). Quartz is the most stable phase and has the lowest solubility, whereas amorphous silica is the least stable phase and has the highest solubility. Thus quartz and amorphous silica must represent two extreme cases of silica dissolution–precipitation equilibria in hydrothermal systems. The solubility of other silica phases will be in between the two extreme solubilities. The residence time for geothermal reservoir fluid is high enough to reach equilibrium with quartz. Therefore, we will deal only with the solubility of quartz in this work.

Theoretical considerations to explain quartz solubility results have been proposed by many workers (Jasmund, 1952; Brady, 1953; Frederickson and Cox, 1954; Franck, 1956; Mosebach, 1957; Greenberg, 1958; Wood, 1958; Wasserburg, 1958; Wasserburg and Wood, 1958; Smith, 1958; Kitahara, 1960; Laudise and Ballman, 1961 and others). Volosov et al. (1972) derived empirical equations for first and second dissociation constants for silicic acid as function of temperature only from a compilation of experimental solubility data in the temperature range 25–350°C. Seward (1974) determined experimentally the first ionization constant (K_1) of silicic acid from quartz solubility in borate buffer solution at 350°C. Iler (1979) reviewed the chemistry of silica. Walther and Helgeson (1977) formulated a semi-theoretical basis for the solubility in water of α -quartz and other polymorphic forms of silica at conditions ranging from 0 to 600°C and pressures up to 500 MPa. Fournier (1983) presented an empirical formula to express quartz solubility in terms of temperature and density of water, indirectly taking care of the activity coefficient and pressure effect terms. Ragnarsdóttir and Walther (1983) studied the pressure sensitivity of quartz solubility at 250°C.

The work of Rimstidt and Barnes (1980) on the kinetics of silica dissolution–precipitation is widely accepted. Recently, Dove and coworkers (Dove and Crerar, 1990; Dove and Elston, 1992) studied the effect of temperature and pH on the kinetics of quartz dissolution in a wide variety of electrolyte solutions. Knowledge of quartz dissolution kinetics is helpful in understanding the time required to reach the dissolution–precipitation equilibrium. Here we are concerned only with the equilibrium model (i.e. water and quartz are always in equilibrium), and will therefore not pay much attention to the kinetics of quartz dissolution.

The experimental measurement of solubility constants over wide ranges of temperature and pressure for all the reactions in an aqueous system is a tedious job due to the slowness of equilibration and the difficulty in determining the actual species in the solution (Hemley et al., 1980). An alternative approach is the chemical thermodynamic calculation, presented by Chatterjee (1991) in a very systematic way for geological systems. In his study, Chatterjee uses this approach to study the dissolution–precipitation of quartz in pure water. The dissolution of quartz produces silicic acid, H_4SiO_4 (Mosebach, 1957; Anderson and Burnham, 1967; Busey and Mesmer, 1977), which further dissociates to H_3SiO_4^- and $\text{H}_2\text{SiO}_4^{2-}$ (Greenberg, 1958). The details of the calculation procedure with the chemical reactions considered for the SiO_2 – H_2O system are presented in Appendix A. The geothermal systems have temperatures lower than the α – β phase transition

Table 1
Thermodynamic data for the silica–water system at the standard state ($T = 298.15\text{K}$ and $P = 0.1\text{ MPa}$). The data are taken from Robie et al. (1978) and Naumov et al. (1971).

Substance	Formula weight	Molecular volume (cm^3/mol)	S_{0298} (J/mol)	$\Delta H_{0F, 298}$ (J/mol)	H_{0298} (J/mol)	$\Delta G_{0F, 298}$ (J/mol)	G_{0298} (J/mol)	C_{p0} (J/mol K)
$\text{H}_2\text{O}_{\text{liq}}$	18.015	18.069	69.92	–285830	13293	–137141	–7562.59	–
$\text{SiO}_{2(\text{cr})}$	60.085	22.688	41.46	–910700	6916	–856288	–5445.30	$= 44.603 + 3.7754 \cdot 10^{-2} T - 1.0018 \cdot 10^6 T^{-2}$
H_4SiO_4	96.115	–	18.00	–1462141	–	–1308000	–	$= 0.719648 T$
H_3SiO_4^-	95.107	–	179.50	–1426158	–	–1253945	–	$= -0.17528 T$
$\text{H}_2\text{SiO}_4^{2-}$	94.099	–	112.50	–1395520	–	–1187001	–	$= -0.9414 T$
OH^-	17.007	–	–10.71	–230025	–	–157328	–	$= -0.46024 T$

of quartz at 571°C (Robie et al., 1978). Thus we will be dealing with α -quartz in the formulation of silica solubility.

Table 1 presents the thermodynamic data set for the quartz-water system, which were taken from Robie et al. (1978) and Naumov et al. (1971). The thermodynamic data for water also reported by Robie et al. (1978) are applicable for 0.1 MPa and any temperature. In geothermal systems both temperature and pressure vary, so these data are of limited use. On the other hand, the steam tables contain very accurate thermodynamic data for water, taking the triple point as standard state (Haar et al., 1984). The thermodynamic state functions are independent of path, so the thermodynamic data (such as enthalpy and entropy) for liquid water at any temperature and pressure can be calculated from the steam tables, converting them to the standard state, 0.1 MPa and 298.15 K.

The approach for creating internal consistency in the thermodynamic data set for solid phase minerals was developed by Berman and Brown (1985), Powell and Holland (1985), Berman (1988), Holland and Powell (1990), and Saxena (1992). Richet et al. (1982) measured the thermodynamic properties of many silica phases up to 2000 K. Recently, Swamy et al. (1994) developed an internally consistent thermodynamic data set for many solid silica phases. The pressure dependence of the Gibbs free energy for quartz used in our calculation was taken from their work. The pressure dependence of quartz for the temperature and pressure range

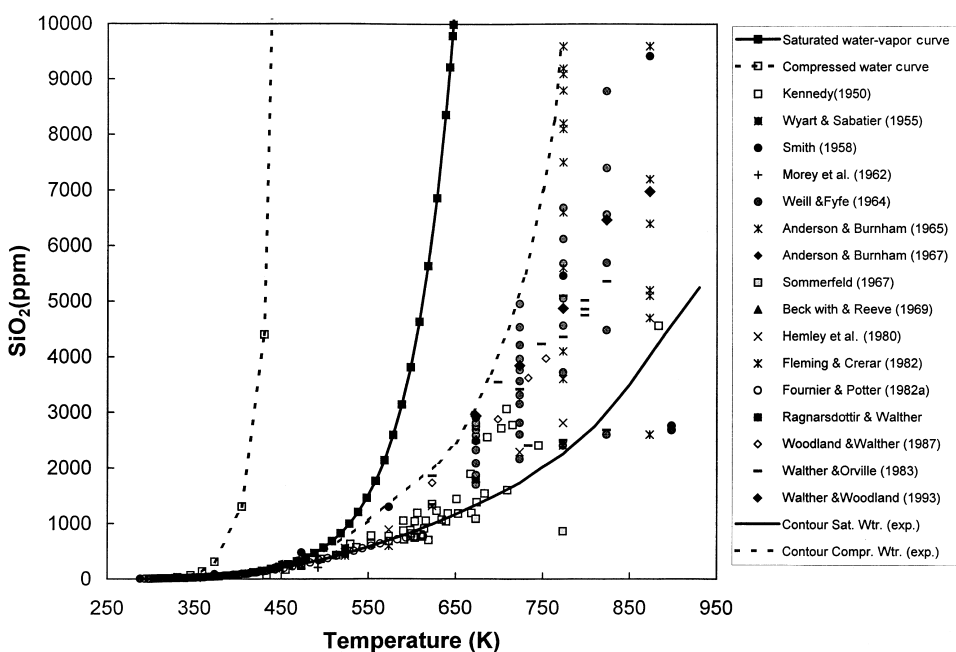


Fig. 2. Experimental and theoretical quartz solubility data. The theoretical curves are for the two extreme cases: (a) when the vessel is completely filled with water, and (b) when it is filled just enough to make the total specific volume equal to the critical volume.

Table 2
A compilation of quartz solubility literature for the $\text{SiO}_2\text{--H}_2\text{O}$ system

Reference	Determination method	Temperature range (in °C)	Pressure range (in MPa)	No. of data	Observations
Kennedy (1950)	1 ^a	Up to 560	Up to 175	44	The data taken were those showing an increase in solubility with temperature
Wyart and Sabatier (1955)	–	400	50–200	4	–
Smith (1958)	–	25–700	0.1–531	8	Extrapolated data
Morey et al. (1962)	2 ^b	Up to 240	Up to 3.3	11	The runs at 100 MPa are not included, because the pressure is achieved by pumping water in the reaction vessel
Weill and Fyfe (1964)	1 ^a	400–625	100–400	41	The only data considered were these with sufficient run time to achieve equilibrium
Anderson and Burnham (1965)	1 ^a	500–900	100–1000	79	The initial amount of water was such that there was only water in the vessel under all conditions of pressure and temperature
Anderson and Burnham (1967)	1 ^a	700	400	2	There are two data at the same conditions of pressure and temperature with changing run time
Sommerfeld (1967)	1 ^a	400–500	100	2	There were 12 runs each for 400 and 500°C and around 100 MPa. Here we averaged the data
Beckwith and Reeve (1969)	–	25	0.1	1	They presented only one datum for quartz solubility (11 ppm) in pure water. There are some more data relative to buffering the solution
Hemley et al. (1980)	2 ^b	250–500	100	7	Their determinations are more reliable as they were made for longer time periods
Fleming and Crerar (1982)	–	Up to 300	–	5	The determinations were made in vapor-saturated liquid water
Fournier and Potter (1982a)	2 ^b	20–374	–	51	Revised data along the water–vapor saturation curve. There is a decrease in solubility above 340°C. Probably, the data for the vapor phase need to be corrected for the proportion of vapor and liquid present in the reaction vessel
Woodland and Walther (1987)	3 ^c	350–480	–	–	Averaged data from Walther and Woodland (1993)
Ragnarsdóttir and Walther (1983)	3 ^c	250	25–100	3	Pressure-dependence study. $\Delta P = \pm 1$ MPa, $\Delta T = \pm 3^\circ\text{C}$
Walther and Orville (1983)	3 ^c	350–500	100–200	19	$\Delta P = \pm 1$ MPa, $\Delta T = \pm 5^\circ\text{C}$
Walther and Woodland (1993)	3 ^c	400–600	200	5	–

^a Weight loss.

^b Quenching bomb to room temperature.

^c Solution extraction at the specified temperature and pressure.

along the water–vapor saturation curve has little significance, but when the reaction vessel is completely filled with water, pressure plays a very important role (Ragnarsdóttir and Walther, 1983).

Fig. 2 shows the theoretically calculated quartz solubility curves for the two extreme cases, when the vessel (bomb) is completely filled with water at room temperature (25°C) and pressure of 0.1 MPa and when it is filled just enough for the total specific volume to be equal to the critical volume of water. It can be observed that these curves are exponential. At low temperatures the solubility gradient is too small to be used as a geothermometer, but is very high in the higher temperature range. The use of silica geothermometers might have been limited to the temperature range 120–250°C because of this reasoning (Fournier, 1977; Henley et al., 1984).

4. Experimental quartz solubility data

There exists a vast literature on the experimental determination of silica solubility over a wide range of experimental conditions of pressure, temperature, pH and presence of other minerals (Fournier, 1973; Fournier and Potter, 1982a, 1982b; Bennett, 1991; Dove and Elston, 1992; Gratz and Bird, 1993). Here we are only concerned with the quartz solubility in pure water with varying temperature. For the two extreme cases considered here, pressure is not an independent variable and is controlled by temperature. Table 2 presents a summary of quartz solubility data compiled from the literature.

The solubility determination has been performed using one of the three methods (Fournier and Potter, 1982b): (1) weight loss of quartz in a known amount of water, (2) chemical analysis of dissolved silica remaining in solution after rapid quenching and opening of the reaction vessel, and (3) chemical analysis of dissolved silica in a small amount of solution extracted from the reaction solution while the vessel is maintained at the specified temperature and pressure.

All the solubility data are also plotted together with the theoretical solubility curves in Fig. 2. As mentioned earlier, the theoretical curves are plotted for two extreme cases, when the vessel (bomb) is completely filled with water at room temperature (25°C) and a pressure of 0.1 MPa, and when it is filled just enough to make the total specific volume equal to the critical volume of water. Thus, the experimentally determined quartz solubility data in pure water should lie between these two curves. It can be observed, however, that the data fall below the curve for water–vapor saturation, but the behavior of all the experimental data is approximately the same as that of the theoretical curves.

The values of pressure and temperature for all the solubility experiments, together with the theoretical P – T curves for the two extreme cases, are plotted in Fig. 3. All the experimental pressure and temperature data lie between the two theoretical curves. The details of pressure and temperature control during the experimental solubility measurements are not described clearly in the literature. In absence of such details, and taking into account that all the experimental pressure

and temperature data points fall between the theoretical curves, it can be summarized that the pressure and temperature during all these studies were controlled by the amount of water in the reaction vessel. Under these circumstances the experimental solubility data should also lie between the theoretical curves in Fig. 2.

5. Discrepancy between theoretical and experimental solubility data

To understand the differences between the theoretical and experimental solubility data we consider two fundamental aspects: (1) *the thermodynamic data set for all the species* and (2) *the details of the measurement methods and experimental conditions to achieve equilibrium between solid and liquid phases*. Dissolved silica in natural water behaves like a weak acid (Roller and Ervin, 1940; Ryzhenko, 1967; Seward, 1974; Arnórsson, 1975), so silicic acid is the dominant specie in aqueous solution (Weill and Fyfe, 1964; Busey and Mesmer, 1977). The thermodynamic data for silicic acid therefore play an important role in the

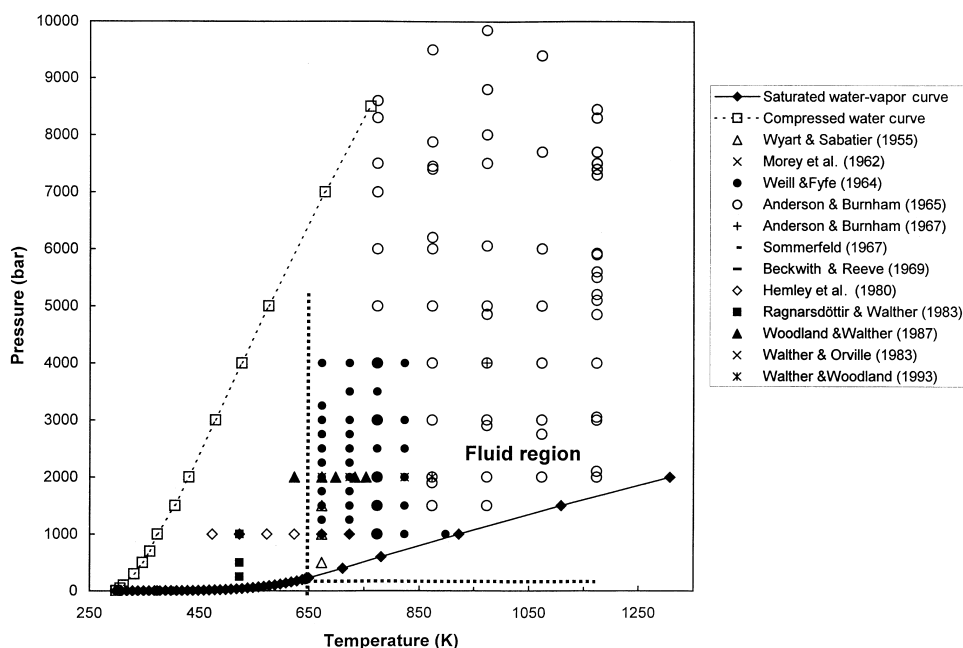


Fig. 3. The pressure and temperature values for all the experimental determinations of quartz solubility, together with theoretical values for the two extreme cases of the amount of water in order to make sure that water phase only exists at high temperatures (i.e. when the reaction vessel is just filled with water equal to the critical volume and when it is completely filled at room temperature). The fluid (supercritical) region is marked with dashed lines. The experimental points lie within the compressed liquid region even in the fluid region.

solubility calculations. One way of obtaining consistency between the theoretical and experimental solubilities is by adjusting the thermodynamic data for silicic acid.

The experimental determination of quartz solubility also needs looking into. Natural surface waters have much higher silica concentrations than determined by the solubility of quartz (Okamoto et al., 1957). This is an indirect indication of the slowness of silica solubility equilibria. Therefore, equilibrium between water and quartz at room temperature requires very long-run experiments without supersaturating the solution at any instant, in order to prevent equilibration with other silica phases. Morey et al. (1962) mentioned that some researchers obtained values for quartz solubility at room temperature that are very close to theoretically calculated values (Brisco et al., 1936/1937; van Lier et al., 1960). It was argued that they got higher values because very fine quartz powder was used in the experiments. It is true that equilibrium can be achieved slightly earlier with fine quartz but the final concentration will be controlled by the quartz solubility equilibrium. A small amount of amorphous silica initially present in the quartz could strongly influence the silica concentration in the solution. The recent data by many workers (Fournier and Potter, 1982a, 1982b; Fleming and Crerar, 1982) show that the solubility of quartz at 25°C and 0.1 MPa is 6.6 ± 1 ppm.

Most of the solubility determinations were performed with the weight loss method or by rapid quenching of reaction vessels to room temperature. Anderson and Burnham (1967) observed the formation of amorphous silica precipitate on quenching the reaction vessel. Walther and Orville (1983) also pointed out that numerous problems might occur because minerals and solutions remain in contact during the quenching. When extremely low solubility is measured even very minor reactions between solution and primary solid phase on quench may significantly change the relative concentrations of cations compared to those of a solution at high pressure and temperature.

Another important point, which is mostly ignored in experimental quartz solubility determinations, is the amount of water and vapor in the reaction vessel. Minerals such as quartz are only soluble in the liquid phase. Thus, the solution after quenching also has condensed vapor, which indirectly modifies the concentration of silica in solution. The theoretically calculated multipliers to correct the silica concentration in the solution at specified temperature and pressure are shown in Table 3. For example, if there is 10% water and 90% vapor by volume in the reaction vessel at a temperature of 370°C (along the water–vapor saturation curve), the concentration measured with the weight loss or quenching of reaction vessel methods should be multiplied by 5 to obtain the concentration in solution at 370°C. On other hand, when there is 90% water in the reaction vessel at the same temperature, the measured concentration needs to be multiplied by 1.05. Therefore, there will be an error of 5% even for experiments with 90% liquid at this temperature. At a specified pressure and temperature along the water–vapor saturation curve, there could be any amount

of water from 0 to 100%. In other words, knowledge of the proportion of water and vapor is vital to solubility determination along the saturation curve.

In summary, the application of silica solubility in understanding hydrothermal system characteristics is based on creating a consistent experimental database for solubility and thermodynamic data for a wide range of temperature and pressure. The low temperature experimental solubility data along the water–vapor saturation curve are probably reasonably accurate, but the high temperature data need revision. Undissociated silicic acid is dominant specie in aqueous solution and the thermodynamic data for solid silica phases have been checked for internal consistency (Swamy et al., 1994). The Gibbs energy of silicic acid is taken to $-1,308,000$ J/mol as was reported by Robie et al. (1978). It gives the solubility of quartz to be 6.6 ppm at 25°C and 0.1 MPa.

Fig. 2 also shows the theoretical solubility curves. It can be observed that the experimental solubility data along the saturation curve below 475 K lie on the theoretical curve. But the high temperature solubility data are still far below the theoretical curve. Therefore there is a need for internally consistent thermodynamic data, as well as for the revision of high temperature solubility data. Nevertheless, here we will use the theoretical curves in elucidating the concepts behind the quartz geothermometers.

6. Quartz geothermometer

The development of the silica geothermometer has been a continuous process that started with the pioneering work of White et al. (1956). The work of Fournier and his collaborators (Fournier and Rowe, 1962, 1966; Morey et al., 1962, 1964; Fournier, 1973, 1983; Fournier and Potter, 1982a) is definitely a great

Table 3

Values of the correction factor for silica concentration determined by the experimental methods, weight loss or quenching-of-reaction-vessel, for different amounts of water and vapor in the reaction vessel using steam tables (Haar et al., 1984)

<i>T</i> (°C)	<i>P</i> (MPa)	<i>V</i> _{liq} (cm ³ /g) ^a	<i>V</i> _{vap} (cm ³ /g) ^b	Concentration multiplier factor (for amount of water in % by vol%)				
				10%	30%	50%	70%	90%
100	0.101	1.0434	1673.600	1.00561	1.00145	1.00062	1.00027	1.00007
150	0.476	1.0904	392.860	1.02498	1.00648	1.00278	1.00119	1.00031
200	1.554	1.1564	127.320	1.08174	1.02119	1.00908	1.00389	1.00101
250	3.974	1.2515	50.111	1.22476	1.05827	1.02497	1.01070	1.00277
300	8.584	1.4037	21.667	1.58306	1.15116	1.06478	1.02776	1.00720
350	16.521	1.7401	8.812	2.77722	1.46076	1.19747	1.08463	1.02194
370	21.030	2.2068	4.993	4.97781	2.03128	1.44198	1.18942	1.04911

^a *V*_{liq}: Specific volume of liquid.

^b *V*_{vap}: Specific volume of vapor.

achievement in creating empirical equations from the experimental solubility data. The quartz geothermometer derived through the regression of experimental solubility data to a polynomial by Fournier and Potter (1982a) is widely accepted in the geothermal community (Verma and Santoyo, 1997). However, the higher temperature solubility data reported by Fournier and Potter (1982a) are definitely affected by the amount of vapor in the reaction vessel, because there is a decrease in solubility with increase in temperature. The experimental solubility data by Fournier and Potter (1982a) and Ragnarsdóttir and Walther (1983), together with theoretical solubility data for the two extreme cases for the amount of water in the reaction vessel, are plotted as the logarithmic concentration of silica versus temperature in Fig. 4. There is a good linear correlation for the calculated saturated water solubility data (i.e. for total specific volume equal to the critical specific volume of water, $3.106 \text{ cm}^3/\text{g}$). Although a line is also fitted for the case of compressed liquid data (i.e. when the vessel was completely filled with water at room temperature), a quadratic polynomial fit could be better in this case. The equation for the straight line for quartz solubility along the water vapor saturation line is the following:

$$\log \text{SiO}_2 \text{ (ppm)} = 0.0179T \text{ (K)} - 4.3143$$

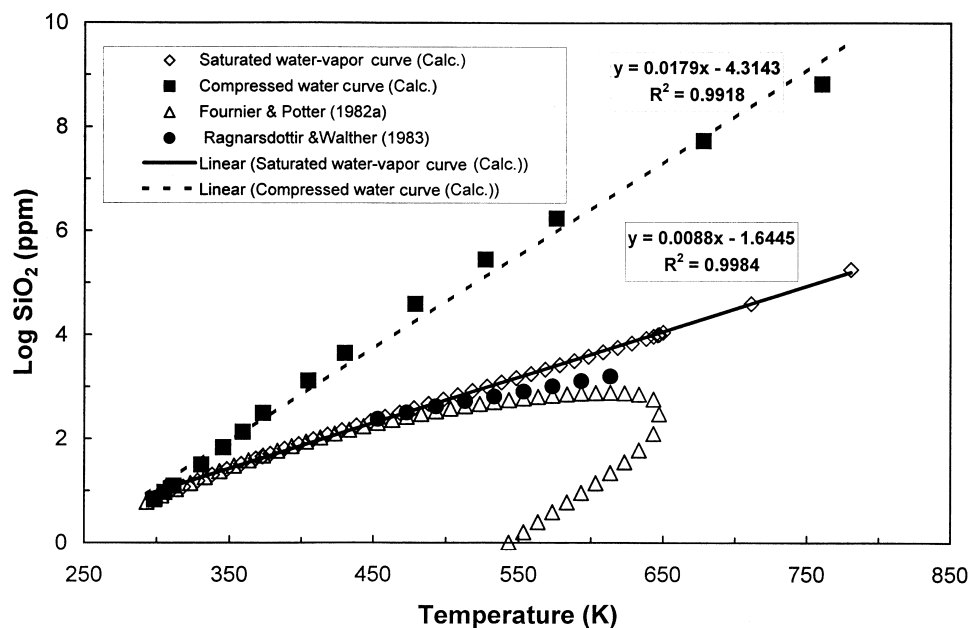


Fig. 4. The relation between quartz solubility data and temperature. There is a very good linear correlation for the logarithmic of solubility data with temperature following the water–vapor saturation path. The revised data by Fournier and Potter (1982a) and Ragnarsdóttir and Walther (1983) are also shown. The data of Ragnarsdóttir and Walther (1983) are closer to the theoretical data at higher temperatures than those of Fournier and Potter (1982a).

Similarly, the equation for the second extreme case is:

$$\log \text{SiO}_2 \text{ (ppm)} = 0.0088T \text{ (K)} - 1.6445$$

The experimental solubility data at lower temperatures are close to the calculated values. Above 425 K the solubilities diverge. A very tentative explanation for this disagreement is that there may not be complete equilibrium between water and quartz; alternatively, the data could be affected by the amount of vapor in the reaction vessel and/or re-equilibration during quenching of the reaction vessel at higher temperatures.

Ragnarsdóttir and Walther (1983) presented revised solubility data for quartz in saturated water in the temperature range 180–340°C. These data indicate higher solubility in the high-temperature region than those of Fournier and Potter (1982a), but are still far below the theoretical data.

In geothermal reservoirs the pressure is generally lower than the (static) water–vapor pressure. It can be considered that the geothermal reservoir fluid follows the saturated water–vapor curve. Thus, the equation for the saturated water can be applied for geothermal fluid to estimate reservoir temperature. The silica concentration in the total discharge fluid is normally used in estimating reservoir temperature. As we know, silica is only soluble in the liquid phase and it is difficult to predict the proportion of vapor and liquid from the discharge fluid characteristics. Therefore, it is a fundamental limitation to its application that one has to determine the amount of vapor and water in the reservoir by other methods. This limitation should not significantly affect the estimation of reservoir temperature by the quartz solubility equation for temperatures lower than 150°C and in the range 150–250°C the correction will be moderate; however it will be highly significant at higher temperatures.

7. Reservoir temperature estimations

The silica geothermometer has been applied extensively to estimate geothermal reservoir temperature from the silica concentration of the fluid obtained from natural manifestations and drilled wells. Unfortunately, the predicted temperatures generally show a wide dispersion even when applying a single geothermometer to all the wells in a geothermal field (Verma and Santoyo, 1997). Many explanations have been proposed for these discrepancies, including gain or loss of steam phase in the reservoir, mixing of different types of fluids, re-equilibration during ascension to the surface, precipitation–dissolution, etc. (Fournier and Truesdell, 1974).

There could always be some silica concentration data that satisfy a given geothermometer equation, so that it is not a proper approach to validate some geothermometer equation through application to a specific data set. In the case of silica there is still a deficiency in the experimental and theoretical information needed to understand geological processes through its fluid chemistry.

Recently, Verma and Santoyo (1997) improved the silica geothermometer equation proposed by Fournier and Potter (1982a) and applied it for demonstrating a reasonable agreement between the estimated and measured reservoir temperatures in the Cerro Prieto geothermal reservoir. They took the chemical data for the reservoir liquid from Fausto et al. (1979). One way to calculate deep-liquid composition is from reservoir enthalpy and temperature. Probably, Fausto et al. (1979) used the silica temperature for this purpose. They do not state clearly the procedure that they used for the reservoir fluid concentration calculation. In the same proceedings, Truesdell et al. (1979) presented results indicating that the silica temperature in all the wells in Cerro Prieto is always lower than the measured, NaKCa and enthalpy temperatures.

Verma (1997) presented a two-phase flow approach to calculate the fluid thermodynamic parameters, including chemical speciation, pressure, and temperature in a geothermal reservoir from the parameters measured in the geothermal fluid (vapor and liquid) at the wellhead separator. Using this approach the geothermal reservoir fluid parameters were calculated in well M-19A at Cerro Prieto. The concentration of silica is 666 ppm and the reservoir temperature is 248°C. The data point is shown in Fig. 5. It can be observed that the value is

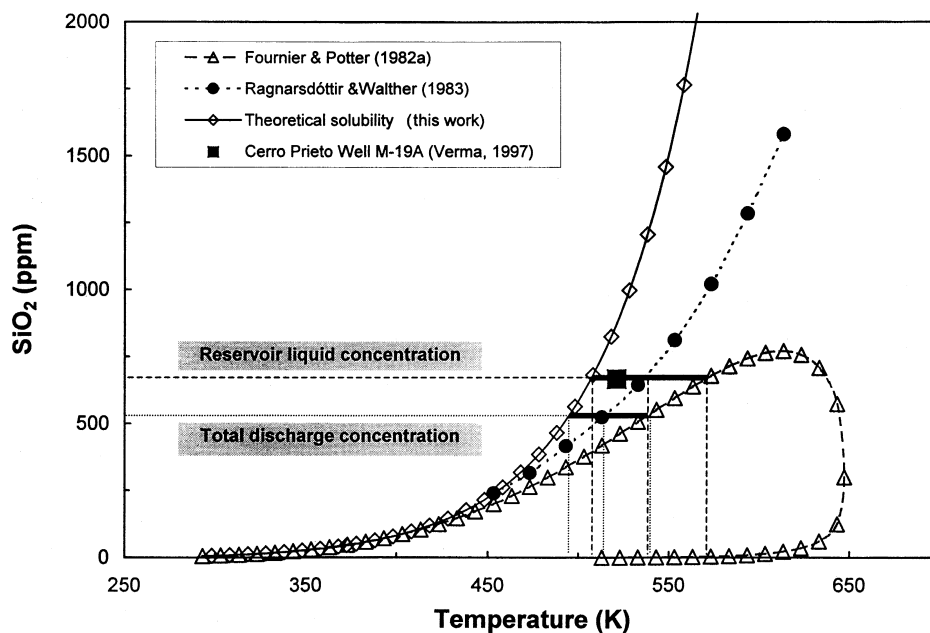


Fig. 5. The calculated concentration of silica in the liquid phase in the reservoir and in the total concentration at wellhead for well M-19A at Cerro Prieto (Verma, 1997). The reservoir temperature is 248°C. Therefore, the reservoir concentration of silica is higher than the experimental solubility values reported by Fournier and Potter (1982a, 1983), but lower than the thermodynamically calculated value.

higher than the quartz solubility reported by Ragnarsdóttir and Walther (1983), but lower than the thermodynamically calculated solubility.

If we apply the silica geothermometers based on these three data sets for quartz solubility (i.e. using data from Fournier and Potter, 1982a; Ragnarsdóttir and Walther, 1983 and the data calculated thermodynamically in this study) along the water vapor saturation curve, the reservoir temperatures obtained by these geothermometers for well M-19A will be approximately 295, 260 and 235°C, respectively. Verma (1997) also calculated the vapor fraction in the reservoir as 0.244 by weight. The total discharge concentration of silica at the wellhead will therefore be about 517 ppm (Fig. 5). If we apply the above geothermometers to the total discharge concentration, the reservoir temperatures will be approximately 265, 240 and 220°C, respectively.

It is clear that the dispersion in the calculated temperature values is higher than the errors reported in the experimental solubility and in the thermodynamic data set for this silica-water system. Secondly, the corresponding temperature values for the reservoir fluid and the total discharge concentration of silica show a difference of approximately 30°C in this case, when there is only 22.4% by weight vapor in the reservoir. As we have seen, there could be any amount of vapor from 0 to 100% along the water–vapor saturation curve. An independent estimation of reservoir vapor fraction is therefore essential in the application of silica geothermometry. The two-phase flow approach gives the values of vapor fraction and temperature (Verma, 1997), so the silica solubility data could also be useful to understand the state of silica-water equilibrium.

Similarly, silica-enthalpy mixing models for geothermal systems to estimate subsurface processes such as boiling and/or mixing of different types of waters have been developed by Fournier and Truesdell (1974), Truesdell and Fournier (1977), and Fournier (1977). Arnórsson and Svavarsson (1985) argued for the use of total composition of water and steam to expand and improve geothermometry involving subsurface temperature assessment, and in depicting mixing and boiling processes. In these mixing models the silica concentration is treated as a conservative entity. Verma et al. (1989) pointed out, in the case of the Los Azufres geothermal system, that other conservative species such as Cl^- , $\delta^{18}\text{O}$ and δD do not show mixing trends similar to those predicted by silica. Thus, in the case of silica the dissolution–precipitation or re-equilibration processes are also important, along with boiling and mixing, during the ascent of geothermal fluid towards the surface. Fournier (1989) also reported that the silica solubility at higher temperatures decreases drastically as temperature decreases, so silica might be precipitated from solution as a result of conductive or adiabatic cooling before reaching the surface.

In summary, it is first necessary to improve our theoretical concepts of silica fluid chemistry in order to achieve coherence between the theoretical and experimental solubility data. The relation between the silica concentration and other more conservative geothermal fluid species such as Cl^- , δD , etc. has to be understood. The silica solubility data used by Fournier and Potter (1982a) are probably incorrect at higher temperatures.

8. Conclusions

The chemical thermodynamic approach is a systematic procedure to calculate silica solubility in aqueous solutions. Steam tables are used to obtain the thermodynamic data for water. Knowledge of the PVT characteristics of water is essential in interpreting the high temperature and pressure solubility data. It is concluded that the reaction vessel must contain a greater amount of water than the critical volume of water to maintain a liquid phase (solution) at high temperature and pressure. Similarly, there could be any proportion of water and vapor in the reaction vessel along the water–vapor saturation curve at a specified temperature. In the high-temperature region, the density (or specific volume) values for both water and vapor are of the same order of magnitude. Silica is virtually only soluble in the liquid phase. Thus the vapor correction to the solubility data is significant in the high temperature region along the saturation curve as there can be any amount of water–vapor.

The experimental quartz solubility data are lower than the corresponding calculated values. This could be due to either inaccuracy in thermodynamic data, or could indicate that the solubility data need revision. Silicic acid is the dominant species in silica solutions with the result that the thermodynamic data for silicic acid could in principle affect the solubility data. It appears certain that the solubility data along the water–vapor saturation curve need re-evaluation at high temperature.

For a reliable application of silica chemistry in hydrothermal systems it is necessary to attain consistency between theoretical and experimental solubility data, to develop independent methods for calculating vapor fraction in the reservoir, and to apply chemical thermodynamic concepts for evaluating the effects of buffering a solution on silica chemistry. The silica concentration in well M-19A at Cerro Prieto is higher than the experimental quartz solubility, but is lower than the calculated solubility.

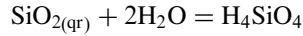
Acknowledgements

This work was carried out under the project MEX/8/022 financed by the IAEA, Vienna, for 1997–98. The author appreciates the constructive comments and suggestions from Prof. Halldor Armannsson and an anonymous reviewer, which contributed considerably in improving the manuscript. This paper is dedicated to a great friend and pioneer geochemist, Dr. Franco D'Amore, who died on 28th March, 1999. He will always be remembered for his excellent contribution to our understanding of the gas geochemistry of geothermal systems.

Appendix A. The chemistry of silica

Many workers (Seward, 1974; Iler, 1979 and others) have presented the

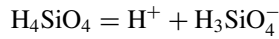
chemical equations involved in the silica-water system. The dissolution of silica is considered to result in the formation of silicic acid according to the following reaction:



The solubility constant for the reaction is:

$$K_{\text{qr}} = \exp\left(\frac{-\Delta G_{\text{F}}^{T,P}}{RT}\right) = \frac{[\text{H}_4\text{SiO}_4]}{[\text{SiO}_2][\text{H}_2\text{O}]^2} = [\text{H}_4\text{SiO}_4] \quad (\text{A1})$$

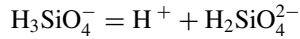
where $\Delta G_{\text{F}}^{T,P}$ is the Gibbs' free energy of formation for the reaction at any temperature (T) and pressure (P), R is the gas constant, and the terms inside the [] indicate the molar concentrations of the species. Thus, the activity coefficient is considered equal to one for all the species, and water and solid are considered as pure phases. In other words their activity is taken as one. The silicic acid dissociates to form hydrogen ion and H_3SiO_4^-



The acid dissociation constant is:

$$K_1 = \frac{[\text{H}^+][\text{H}_3\text{SiO}_4^-]}{[\text{H}_4\text{SiO}_4]} \quad (\text{A2})$$

The H_3SiO_4^- further loses one proton:



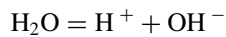
The second acid dissociation constant can be expressed as:

$$K_2 = \frac{[\text{H}^+][\text{H}_2\text{SiO}_4^{2-}]}{[\text{H}_3\text{SiO}_4^-]} \quad (\text{A3})$$

The total concentration of dissolved silica is:

$$C_T = [\text{H}_4\text{SiO}_4] + [\text{H}_3\text{SiO}_4^-] + [\text{H}_2\text{SiO}_4^{2-}] \quad (\text{A4})$$

Dissociation of water proceeds according to the reaction:



The water dissociation constant is:

$$K_{\text{W}} = [\text{H}^+][\text{OH}^-] \quad (\text{A5})$$

The proton balance equation is:

$$[\text{H}^+] = [\text{OH}^-] + [\text{H}_3\text{SiO}_4^-] + 2[\text{H}_2\text{SiO}_4^{2-}] \quad (\text{A6})$$

The fractions of silicic species, that lost no proton, one proton and two protons, can be expressed as:

$$\begin{aligned}\alpha_0 &= \frac{1}{1 + \frac{K_1}{[H^+]} + \frac{K_1 K_2}{[H^+]^2}} \\ \alpha_1 &= \frac{\frac{K_1}{[H^+]}}{1 + \frac{K_1}{[H^+]} + \frac{K_1 K_2}{[H^+]^2}} \\ \alpha_2 &= \frac{\frac{K_1 K_2}{[H^+]^2}}{1 + \frac{K_1}{[H^+]} + \frac{K_1 K_2}{[H^+]^2}}\end{aligned}\quad (A7)$$

The values of K , K_1 and K_2 are calculated from the Gibbs' free energy of formation for the corresponding equations. The dissociation constant of water is calculated similarly. Substituting the expressions α_0 , α_1 and α_2 , the following equation is solved using the error-and-trail numeric method

$$\text{func} = \frac{K_W}{[H^+]} + C_T[\alpha_1 + 2\alpha_2] - [H^+] = 0 \quad (A8)$$

Knowing the value of $[H^+]$, the values of α_0 , α_1 and α_2 are calculated according to the above equations. The total dissolved concentration of silicic species is calculated as:

$$C_T = \frac{[H_4SiO_4]}{\alpha_0} \quad (A9)$$

The concentration of the other silicic species $H_3SiO_4^-$ and $H_2SiO_4^{2-}$ is calculated with the following equations:

$$\begin{aligned}[H_3SiO_4^-] &= C_T \alpha_1 \\ [H_2SiO_4^{2-}] &= C_T \alpha_2\end{aligned}\quad (A10)$$

Thus, the concentrations of all the chemical species in a solution of silica in water can be calculated. The dissolved silica concentration in the solution is expressed as the concentrations of all the dissolved silicic species.

References

- Alexander, G.B., Heston, W.M., Iler, R.K., 1954. The solubility of amorphous silica in water. *J. Phys. Chem* 58, 453–455.
- Anderson, G.M., Burnham, C.W., 1965. The solubility of quartz in supercritical water. *Amer. J. Sci* 263, 494–511.
- Anderson, G.M., Burnham, C.W., 1967. Reactions of quartz and corundum with aqueous chloride and hydroxide solutions at high temperatures and pressures. *Amer. J. Sci* 265, 12–27.
- Arnórsson, S., 1970. Underground temperatures in hydrothermal areas in Iceland as deduced from the silica content of the thermal water. *Geothermics, Spec. Issue* 2, 536–541.
- Arnórsson, S., 1975. Application of the silica geothermometer in low temperature hydrothermal areas in Iceland. *Amer. J. Sci* 275, 763–784.
- Arnórsson, S., 1985. The use of mixing models and chemical geothermometers for estimating underground temperatures in geothermal systems. *J. Volc. Geother. Res* 23, 299–335.
- Arnórsson, S., Svavarsson, H., 1985. Application of chemical geothermometry to geothermal exploration and development. *Geotherm. Resour. Coun. Trans* 9, 293–297.
- Beckwith, R.S., Reeve, R., 1969. Dissolution and deposition of monosilicic acid in suspensions of ground quartz. *Geochim. Cosmochim. Acta* 33, 745–750.
- Bennett, P.C., 1991. Quartz dissolution in organic-rich aqueous systems. *Geochim. Cosmochim. Acta* 55, 1781–1797.
- Berman, R.G., 1988. Internally consistent thermodynamic data for minerals in the system $\text{Na}_2\text{O}-\text{K}_2\text{O}-\text{CaO}-\text{MgO}-\text{FeO}-\text{Al}_2\text{O}_3-\text{SiO}_2-\text{TiO}_2-\text{H}_2\text{O}-\text{CO}_2$. *J. Petrol* 29, 445–522.
- Berman, R.G., Brown, T.H., 1985. Heat capacity of minerals in the system $\text{Na}_2\text{O}-\text{K}_2\text{O}-\text{CaO}-\text{MgO}-\text{FeO}-\text{F}_2\text{O}_3-\text{Al}_2\text{O}_3-\text{SiO}_2-\text{TiO}_2-\text{H}_2\text{O}-\text{CO}_2$: representation, estimation, and high temperature extrapolation. *Contrib. Mineral Petrol* 89, 168–183.
- Böðvarsson, G., 1960. Exploration and exploitation of natural heat in Iceland. *Bull. Volcanol. Ser* 2 (23), 241–250.
- Böðvarsson, G., Pálmason, G., 1961. Exploration of subsurface temperatures in Iceland. In: *Proc. U.N. Conf. New Sources Energy. G/24, Rome*, 82–90.
- Brady, E.L., 1953. Chemical nature of silica carried by steam. *J. Phys. Chem* 57, 706–710.
- Brisco, H.V.A., Mathews, J.W., Holt, P.E., Sanderson, P.M., 1936. Some new characteristic properties of certain industrial dusts. *Inst. Min. Metall. Trans* 46, 291–302.
- Busey, R.H., Mesmer, R.E., 1977. Ionization equilibria of silicic acid and polysilicate formation in aqueous sodium chloride solutions at 300°C. *Inorg. Chem* 16, 2444–2450.
- Chatterjee, N.D., 1991. *Applied Mineralogical Thermodynamics*. Springer-Verlag, New York, p. 322.
- D'Amore, F., Fancelli, R., Caboi, R., 1987. Observation on the application of chemical geothermometers to some hydrothermal systems in Sardinia. *Geothermics* 16, 271–282.
- Dove, P.M., Crerar, D.A., 1990. Kinetics of quartz dissolution in electrolyte solutions using a mixed flow reactor. *Geochim. Cosmochim. Acta* 54, 955–969.
- Dove, P.M., Elston, S.F., 1992. Dissolution kinetics of quartz in sodium chloride solutions: analysis of existing data and a rate model for 25°C. *Geochim. Cosmochim. Acta* 56, 4147–4156.
- Fausto, J.J., Sánchez, A., Jiménez, M.E., Esquer, I., Ulloa, F., 1979. Geoquímica hidrotermal del campo geotérmico de Cerro Prieto. *Second Symp. Cerro Prieto Geothermal Field, Mexicali, Baja California*, 199–223.
- Fleming, B.A., Crerar, D.A., 1982. Silicic acid ionization and calculation of silica at elevated temperature and pH. Application to geothermal fluid processing and reinjection. *Geothermics* 11, 15–29.
- Fournier, R.O., 1973. Silica in thermal waters: laboratory and field investigation. In: *Proc. Symp. Hydrogeochem. Biochem., Tokyo, Japan, vol. 1, Hydrogeochem., The Clarke Co*, 122–138.
- Fournier, R.O., 1977. Chemical geothermometers and mixing models for geothermal systems. *Geothermics* 5, 41–50.
- Fournier, R.O., 1983. A method of calculating quartz solubilities in aqueous sodium chloride solutions. *Geochim. Cosmochim. Acta* 47, 579–586.

- Fournier, R.O., 1989. The solubility of silica in hydrothermal solutions: practical applications. Lectures on Geochemical Interpretation of Hydrothermal Waters. Report 10, UNU Geothermal Training Programme, Iceland, 21–41.
- Fournier, R.O., Marshall, W.L., 1983. Calculation of amorphous silica solubilities at 25 to 300°C and apparent cation hydration numbers in aqueous salt solutions using the concept of effective density of water. *Geochim. Cosmochim. Acta* 47, 587–596.
- Fournier, R.O., Potter Jr II, R.W., 1982a. A revised and expanded silica (quartz) geothermometer. *Geotherm. Resour. Counc. Bull* 11, 3–12.
- Fournier, R.O., Potter Jr II, R.W., 1982b. An equation correlating the solubility of quartz in water from 25 to 900°C at pressures up to 10,000 bars. *Geochim. Cosmochim. Acta* 46, 1969–1973.
- Fournier, R.O., Rowe, J.J., 1962. The solubility of cristobalite along the three-phase curve, gas plus liquid plus cristobalite. *Am. Mineralogist* 47, 897–902.
- Fournier, R.O., Rowe, J.J., 1966. Estimation of underground temperatures from silica content of water from hot springs and wet-steam wells. *Amer. J. Sci* 264, 685–697.
- Fournier, R.O., Truesdell, A.H., 1970. Geochemical indicators of subsurface temperature applied to hot spring waters of Yellowstone National Park, Wyoming, USA. *Geothermics, Spec. Issue* 2, 529–535.
- Fournier, R.O., Truesdell, A.H., 1974. Geochemical indicators of subsurface temperature, part II. estimation of temperature and fraction of hot water mixed with cold water. *U.S. Geol. Survey J. Res* 2, 263–270.
- Franck, E.U., 1956. Zur Löslichkeit fester Stoffe in verdichteten Gasen. *Zeitschr. Phys. Chemie* 6, 345–355.
- Frederickson, A.F., Cox Jr, J.E., 1954. Mechanism of solution of quartz in pure water at elevated temperatures and pressures. *Am. Mineralogist* 39, 886–900.
- Gíslason, S.R., Heaney, P.J., Veblen, D.R., Livi, K.J.T., 1993. The difference between the solubility of quartz and chalcedony: the causes. *Chem. Geol* 107, 363–366.
- Gíslason, S.R., Heaney, P.J., Oelkers, E.H., Schott, J., 1997. Kinetic and thermodynamic properties of moganite, a novel silica polymorph. *Geochim. Cosmochim. Acta* 61, 1193–1204.
- Gratz, A.J., Bird, P., 1993. Quartz dissolution: negative crystal experiments and a rate law. *Geochim. Cosmochim. Acta* 57, 965–976.
- Greenberg, S.A., 1958. The nature of silicate species in sodium silicate solutions. *J. Amer. Chem. Soc* 80, 6508–6511.
- Haar, L., Gallagher, J.S., Kell, G.S., 1984. NBS/NRC Steam Tables: Thermodynamic and Transport Properties for Vapor and Liquid States of Water in SI Units. Hemisphere, New York 320 pp.
- Hemley, J.J., Montoya, W., Marinenko, J.W., Luce, R.W., 1980. Equilibria in the system $\text{Al}_2\text{O}_3\text{-SiO}_2\text{-H}_2\text{O}$ and some general implications for alteration/mineralization processes. *Econ. Geol* 75, 210–228.
- Henley, R.W., Truesdell, A.H., Barton, P.B., Whitney, J.A., 1984. Fluid-mineral equilibria in hydrothermal systems. *Soc. Econ. Geol. El Paso, TX* 1, 267.
- Holland, T.J.B., Powell, R., 1990. An enlarged and updated internally consistent thermodynamic dataset with uncertainties and correlations: the system $\text{K}_2\text{O-Na}_2\text{O-CaO-MgO-MnO-FeO-Fe}_2\text{O}_3\text{-Al}_2\text{O}_3\text{-TiO}_2\text{-SiO}_2\text{-C-H}_2\text{-O}_2$. *J. Metamorphic Geol* 8, 89–124.
- Iler, R., 1979. *The Chemistry of Silica: Solubility, Polymerization, Colloid and Surface Properties, and Biochemistry*. John Wiley, New York 866 pp.
- Jasmund, K., 1952. Thermodynamic behavior of quartz and other forms of silica in pure water at elevated temperatures and pressures with conclusion on their mechanism of solution: a discussion. *J. Geol* 66, 595–596.
- Kennedy, G.C., 1950. A portion of the system silica-water. *Economic Geology* 45, 629–653.
- Kitahara, S., 1960. The solubility of quartz in water at high temperatures and pressures. *Rev. Phys. Chem. Japan* 30, 109–114.
- Krauskopf, K.B., 1956. Dissolution and precipitation of silica at low temperatures. *Geochim. Cosmochim. Acta* 10, 1–26.
- Laudise, R.A., Ballman, A.A., 1961. The solubility of quartz under hydrothermal conditions. *J. Phys. Chem* 65, 1396–1400.
- Levitte, D., Eckstein, Y., 1979. Correlation between the silica concentration and the orifice temperature in the warm springs along the Jordan-Dead-Sea rift valley. *Geothermics* 7, 1–8.

- Mahon, W.A.J., 1966. Silica in hot water discharged from drillholes at Wairakei, New Zealand. *N. Z. J. Sci* 9, 135–144.
- Morey, G.W., Fournier, R.O., Rowe, J.J., 1962. The solubility of quartz in water in the temperature interval from 29 to 300°C. *Geochim. Cosmochim. Acta* 26, 1029–1043.
- Morey, G.W., Fournier, R.O., Rowe, J.J., 1964. The solubility of amorphous silica at 25°C. *J. Geophys. Research* 69, 1995–2002.
- Mosebach, R., 1957. Thermodynamic behaviour of quartz and other forms of silica in pure water at elevated temperatures and pressure with conclusions of their mechanism of solution. *J. Geol* 65, 347–363.
- Naumov, G.B., Ryzhenko, B.N., Khodakovskiy, I.L., 1971. Handbook of Thermodynamic Data. (G.J. Soleimani, Trans.). US Geological Survey, 226–722.
- Okamoto, G., Okura, T., Goto, K., 1957. Properties of silica in water. *Geochim. Cosmochim. Acta* 12, 123–132.
- Pang, Z.-H., Reed, M., 1998. Theoretical chemical thermometry on geothermal waters: problems and methods. *Geochim. Cosmochim. Acta* 62, 1083–1091.
- Powell, R., Holland, T.J.B., 1985. An internally consistent thermodynamic dataset with uncertainties and correlations. Part 1. Methods and a worked example. *J. Metamorphic Geol* 3, 327–342.
- Ragnarsdóttir, K.V., Walther, J.W., 1983. Pressure sensitive “silica geothermometer” determined from quartz solubility experiments at 250°C. *Geochim. Cosmochim. Acta* 47, 941–946.
- Reed, M., Spycher, N., 1984. Calculation of pH and mineral equilibria in hydrothermal waters with application to geothermometry and studies of boiling and dilution. *Geochim. Cosmochim. Acta* 48, 1479–1492.
- Richet, P., Bottinga, Y., Denielou, L., Petitot, J.P., Tequi, C., 1982. Thermodynamic properties of quartz, cristobalite and amorphous SiO₂: drop calorimetry measurements between 1000 and 1800 K and a review from 0–2000 K. *Geochim. Cosmochim. Acta* 46, 2639–2658.
- Rimstidt, J.D., Barnes, H.L., 1980. The kinetics of silica-water reactions. *Geochim. Cosmochim. Acta* 44, 1683–1699.
- Robie, R.A., Hemingway, B.S., Fisher, J.R., 1978. Thermodynamic properties of minerals and related substances at 298.15 and 1 bar (10⁵ Pascals) pressure and higher temperatures. *US Geol. Surv. Bull* 1452, 1–456.
- Roller, P.S., Ervin, G., 1940. The system calcium oxide-silica-water at 30°C. The association of silicate ion in dilute alkaline solution. *J. Am. Chem. Soc* 62, 123–132.
- Ryzhenko, B.N., 1967. Determination of hydrolysis of sodium silicate and calculation of dissociation constants of orthosilicic acid at elevated temperatures. *Geochem. Int* 4, 99–107.
- Saxena, S. 1992. Thermodynamic data: systematics and estimation. In: Saxena, S. (Ed.), *Advances in Physical Geochemistry*. Springer-Verlag, Berlin, pp. 79–97.
- Seward, T.M., 1974. Determination of first ionization constant of silicic acid from quartz solubility in borate buffer solutions to 350°. *Geochim. Cosmochim. Acta* 38, 1651–1664.
- Sigvaldason, G.E., 1966. Chemistry of thermal waters and gases in Iceland. *Bull. Volcanol* 29, 589–604.
- Smith, F.G., 1958. Transport and deposition of the non-sulfide vein minerals. Part VI: Quartz. *Canad. Mineralogist* 5, 210–221.
- Smith, J.M., van Ness, H.C., 1975. *Introduction to Chemical Thermodynamics*. McGraw-Hill Kogakusha, Tokyo, p. 632.
- Sommerfeld, R.A., 1967. Quartz solubility reaction: 400–500°C, 1000 bars. *J. Geophys. Res* 72, 4253–4257.
- Stumm, W., Morgan, J.J., 1981. *Aquatic Chemistry. An Introduction Emphasizing Chemical Equilibria in Natural Waters*. John Wiley, New York 767 pp.
- Swamy, V., Saxena, S.K., Sundman, B., Zhang, J., 1994. A thermodynamic assessment of silica phase diagram. *J. Geophys. Res* 99, 11787–11794.
- Tole, M.P., Ármannsson, H., Pang, Z.-H., Arnórsson, S., 1993. Fluid/mineral equilibria calculations for geothermal fluids and chemical geothermometry. *Geothermics* 22, 17–37.
- Truesdell, A.H., Fournier, R.O., 1977. Procedure for estimating the temperature of a hot water component in a mixed water by using a plot of dissolved silica versus enthalpy. *US Geol. Survey J. Res* 5, 49–52.

- Truesdell, A.H., Thompson, J.M., Coplen, T.B., Nehring, N.L., Janik, C.J., 1979. The origin of the Cerro Prieto geothermal brine. In: *Second Symp. Cerro Prieto geothermal field, Mexicali, Baja California*, 224–240.
- Van Lier, J.H., de Bruyn, P.L., Overbeck, T.G., 1960. The solubility of quartz. *J. Phys. Chem* 64, 1675–1682.
- Verma, M.P., 1997. Thermodynamic classification of vapor and liquid dominated reservoir and fluid geochemical parameter calculations. *Geofísica International* 36, 181–189.
- Verma, M.P., Nieva, D., Santoyo, E., Barragán, R.M., Portugal, E., 1989. A hydrothermal model of Los Azufres geothermal system, Mexico. In: *Proc. 6th International Symposium on Water-Rock Interaction*, 723–726.
- Verma, S.P., Santoyo, E., 1997. New improved equations for Na/K, Na/Li and SiO₂ geothermometers by outlier detection and rejection. *J. Volcanol. Geotherm. Res* 79, 9–23.
- Volosov, A.G., Khodakovskiy, I.L., Ryzhenko, B.N., 1972. Equilibria in the system SiO₂–H₂O at elevated temperatures along the lower three-phase curve. *Geochem. Int* 9, 362–377.
- von Damm, K.L., Bischoff, J.L., Rosenbauer, R.J., 1991. Quartz solubility in hydrothermal seawater: an experimental study and equation describing quartz solubility for up to 0.5 M NaCl solutions. *Amer. J. Sci* 291, 977–1007.
- Walther, J.V., Helgeson, H.C., 1977. Calculation of the thermodynamic properties of aqueous silica and the solubility of quartz and its polymorphs at high pressures and temperatures. *Amer. J. Sci* 277, 1315.
- Walther, J.V., Orville, P.M., 1983. The extraction-quench technique for determination of the thermodynamic properties of solute complexes: application to quartz solubility in fluid mixtures. *Amer. Miner* 68, 731–741.
- Walther, J.V., Woodland, A.B., 1993. Experimental determination and interpretation of the solubility of the assemblage microcline, muscovite, and quartz in supercritical H₂O. *Geochim. Cosmochim. Acta* 57, 2431–2437.
- Wasserburg, G.J., 1958. The solubility of quartz in supercritical water as a function of pressure. *J. Geol* 66, 559–578.
- Wasserburg, G.J., Wood Jr, J.A., 1958. The solubility of quartz at high temperatures and pressures. *Amer. J. Sci* 256, 438.
- Weill, D.F., Fyfe, W.S., 1964. The solubility of quartz in H₂O in the range 1000–4000 bars and 400–500°C. *Geochim. Cosmochim. Acta* 28, 1243–1255.
- White, D.E., Brannock, W.W., Murata, K.J., 1956. Silica in hot-spring waters. *Geochim. Cosmochim. Acta* 10, 27–59.
- Wood Jr, J.A., 1958. The solubility of quartz in water at high temperatures and pressures. *Amer. J. Sci* 256, 40–47.
- Woodland, A.B., Walther, J.V., 1987. Experimental determination of the solubility of the assemblage paragonite, albite, and quartz in supercritical H₂O. *Geochim. Cosmochim. Acta* 51, 365–372.
- Wyart, J., Sabatier, G., 1955. Nouvelles mesures de la solubilité du quartz de la tridymite et de la cristobalite dans l'eau sous pression au-dessus de la température critique. *C.R. Acad. Sci. (Paris)* 240, 1905–1907.
- Xie, Z., Walther, J.V., 1993. Wollastonite + quartz solubility in supercritical NaCl aqueous solutions. *Amer. J. Sci* 293, 235–255.
- Xie, Z., Walther, J.V., 1997. Quartz solubilities in NaCl solutions with and without wollastonite at elevated temperatures and pressures. *Geochim. Cosmochim. Acta* 57, 1947–1955.